EFDA–JET–PR(11)27

D. Zarzoso, M.N.A. Beurskens, L. Frassinetti, E. Joffrin, F.G. Rimini,
E.R. Solano and JET EFDA contributors

ELM Size Analysis in JET Hybrid Plasmas

ELM Size Analysis in JET Hybrid Plasmas

D. Zarzoso, M.N.A. Beurskens, L. Frassinetti, E. Joffrin, F.G. Rimini, E.R. Solano and JET EFDA contributors*

JET-EFDA, Culham Science Centre, OX14 3DB, Abingdon, UK

[1]CEA, IRFM, F-13108 Saint-Paul-lez-Durance, France.
[2]EURATOM-CCFE Fusion Association, Culham Science Centre, OX14 3DB, Abingdon, OXON, UK
[3]Association EURATOM-VR, Alfven Laboratory, Stockolm, Sweden
[4]Asociacion EURATOM-CIEMAT para la Fusion, Madrid, Spain
** See annex of F. Romanelli et al, "Overview of JET Results",*
(23rd IAEA Fusion Energy Conference, Daejon, Republic of Korea (2010)).

Preprint of Paper to be submitted for publication in
Nuclear Fusion

ABSTRACT.
Experimental results are presented in this paper, characterizing the behaviour of type I ELMs for a JET data base of standard ELMy H-mode and hybrid plasmas. Whereas the collisionality scaling published has been reproduced for the new baseline discharges, no clear correlation can be established from the analysis of hybrid scenarios. The ELM losses normalized to the pedestal stored energy for high triangularity hybrid plasmas seem to be significantly larger than the energies for baseline plasmas at similar values of collisionality. For low triangularity hybrid plasmas, the ELM losses are of the same order as those obtained in baseline scenarios. The important scatter of the results seem to be due to the sensitivity of hybrid plasmas to gas-fuelling. Analysis of the ITER-like wall compatibility of hybrid discharges is also reported.

1. INTRODUCTION

The standard ELMy H-mode (baseline scenario) is considered as the reference scenario for future fusion devices like ITER [2]. This mode provides higher confinement compared to the L-mode and has been extensively explored in current fusion devices with X-point geometry such as the JET tokamak. The presence of Edge Localized Modes (ELMs), results in large transient heat loads released onto the Plasma Facing Components (PFCs), which contribute to the overall erosion rate and lifetime of these materials [3, 4]. The control of these loads reveals essential for optimizing the tokamak performance and therefore ensuring the success of future fusion devices. The possible sorting parameter for the ELM size in type I ELMy H-mode plasmas is the pedestal collisionality (ν^*) [5]. Other key parameters that have been identified to have an important eect on the ELM losses are the plasma shape [6], the pedestal width [7], the plasma rotation [8, 9] and the pedestal density [10]. As the ITER operational space is at lower collisionality than current devices, particularly scaling with ν^* is of great concern; an extrapolation of the correlation found in [1] to an ITER-like baseline plasma (15MA) would imply large relative ELM size of 20% of the pedestal stored energy (W_{ped}), or an absolute energy loss of 20MJ, leading to unacceptable heat loads on the divertor target of ITER [11]. Predictions of the behaviour of the full metal wall in ITER are essential. For this reason, an ITER-Like Wall (ILW) is currently being installed in JET and will be tested during the next experimental campaign. Materials studies have shown that the heat load on this facility must not exceed $330\text{kJ}\cdot\text{m}^{-2}$ per ELM [12]. Analysis of previous discharges could provide possible scenarios for ILW exploitation. Parallel to the baseline plasma development, the so-called hybrid scenario is being developed in various devices for use as an alternative scenario for ITER [13, 14]. These operate at lower plasma current (I_p) and increased H_{98} and make up for the lost confinement usually found at the lower current by sustain a larger normalised pressure (β_N). Systematic ELM size scaling experiments have so far not been conducted for these plasmas. Therefore, this paper sets out to compare a new set of baseline and hybrid plasmas in terms of their relative ELM size with respect to the pedestal stored energy and is structured as follows. In section 2 an overview is given of the used methods to determine the pedestal parameters of interest and to obtain the ELM energy

losses. The correlation of ELM size with collisionality is given in section 3 as well as discussions on the ELM energy size and ILW compatibility.

2. METHOD OF ANALYSIS

For the calculation of both the pedestal collisionality and the pedestal stored energy the kinetic proles of density and the temperature at the top of the pedestal are used. The pedestal collisionality and energy have been calculated respectively as [1]

$$\nu^*_{ped} = \frac{13}{1.727 \cdot 10^{17}} q_{95} \frac{R^{5/2}}{a^{3/2}} \frac{n_{e,ped}}{T^2_{e,ped}} \quad (1)$$

$$W_{ped} = \frac{3}{2} k_B \left(n_{i,ped} T_{i,ped} + n_{e,ped} T_{e,ped}\right) V_{plasma} \quad (2)$$

Where k_B is the Boltzmann constant, q_{95} the safety factor, a the minor radius, R the major radius, V_{plasma} the volume of the plasma all obtained from the magnetic equilibrium reconstruction (EFIT). The pedestal temperature and density, $T_{e;ped}$ and $n_{e;ped}$ respectively, are obtained from a modified tanh t performed on the new High Resolution Thomson Scattering (HRTS) data [15]. For the evaluation of T_e and n_e an ELM synchronisation technique is used as described in [16], as for each individual ELM there are very few HRTS measurements (the system measures proles at a rate of 20Hz). The ion density is calculated from the neutrality condition, i.e. $n_e = \sum_s Z_s n_s$, where Z_s and n_s are respectively the atomic number and the density for species s. Under the assumption that carbon is the only impurity present in the tokamak, the neutrality condition yields $n_{i;ped} = \frac{7\text{-}Z_{eff}}{6} n_{e;ped}$. The ion temperature is calculated as $T_{i;ped} = \left.\frac{T_i}{T_e}\right|_{\psi \approx 0.8} T_{e;ped}$, with T_i taken from the core charge exchange diagnostic. The ELM timing is obtained from fast divertor D_α measurements with a 0.1ms sampling rate.

The ELM energy losses are calculated from time resolved measurements of the diamagnetic energy (W_{dia}), which depends only on external magnetic measurements of the poloidal field and the plasma toroidal flux, as well as from the magnetic equilibrium (W_{MHD}). The energy losses ΔW_{dia} and ΔW_{MHD} are calculated in two ways; the first method is the same as described in [16]. The W_{dia} and W_{MHD} time tracers are synchronised to the individual ELMs and the energy drop is calculated using linear ts to the pre- and post-ELM signals. An example is illustrated in Figure 1 for W_{dia}, which shows the signal averaged over many ELMs and synchronised to the ELM crash time, i.e. $t_{ELM} = 0$, for the hybrid Pulse No: 77922 - with ELM frequency of 17.3Hz, $I_p = 1.7$MA, $B_t = 2.3$T.

The second method performs the linear fits to the pre- and post-ELM phases for each of the individual ELM cycles. The average value found by both methods is the same and the second method allows one to obtain the statistical distribution of the ELM losses as shown in Fig.2. This spread is used to indicate the error bars on the ELM energy losses in this study.

The method of linear fits to the pre- and post-ELM phases removes effects around the crash that are generally difficult to measure. They are thought to be partly due to eddy currents induced

in the vacuum vessel and rapid plasma movements on a millisecond timescale which can impact diamagnetic measurements. In this paper a time window of 3 ms after the ELM event is allowed during which the data is not used for the linear fits. For this time window the ELM energy losses as measured with W_{MHD} are consistent with those measured by W_{dia} as illustrated in Figure 3. The diamagnetic measurements are not valid for a few plasmas included in our data base. For this reason, and only for these plasmas, W_{MHD} is used instead for the calculation of the ELM energy losses. All the discharges analysed in this paper exhibit regular type I ELMs of steady frequency. Thus, the parameters used here will not vary signicantly. In addition, the time windows of interest have been chosen outside of any detectable core MHD activity (such as neoclassical tearing modes) and no compound ELMs are considered for the study.

3. ELM SIZE SCALING WITH COLLISIONALITY AND COMPATIBILITY WITH THE ITER-LIKE WALL ON JET

Analysis of the dependence of the ELM losses on ν^*_{ped} as defined in Eq.(1) is carried out within this section. The baseline H-mode plasmas data base covers the following range in dimensionless parameters: $0.001 < \rho^* < 0.002$, $1.5 < \beta_N < 2.2$, $2.5 < q_{95} < 3.8$ for both low and high triangularity plasmas ($\delta = 0.25$ and $\delta = 0.43$). Figure 4 illustrates the ELM losses normalized to the pedestal stored energy as a function of the pedestal collisionality for these plasmas. As a comparison, the measurements of the normalized ELM energy losses from [1] are given. The new and old data present the same general negative correlation between ELM size and collisionality. We have quantified this correlation by means of the linear Pearson correlation coefficient, defined as

$$\rho_{XY} = \frac{\sigma^2_{XY}}{\sigma_X \sigma_Y} \tag{3}$$

where σ^2_{XY} is the covariance between two variables X and Y and σ_X is the standard deviation of X. For the data base of baseline discharges the coefficient has been found to be greater than 0.9. Similar results for the decreasing of the ELM losses have been reproduced recently using nonlinear MHD simulations [17].

For hybrid scenarios, the dimensionless parameters cover the following range: $2.2 < \beta_N < 3$, $3.5 < q_{95} < 4.3$ and again two triangularities: $\delta = 0.22$ and $\delta = 0.38$. The normalized ion Larmor radius and the pedestal collisionality remain in the baseline range. A weaker correlation between the normalized losses and collisionality is observed. In this case, the linear Pearson correlation coefficient is less than 0.09. This is illustrated in Figure 5.

In general, the normalized ELM losses in high triangularity hybrid plasmas are larger than or equal to the losses in baseline plasmas, but the scatter in the data is significantly larger than for the baseline plasmas. For the low triangularity discharges, the losses are of the same order as those obtained in baseline ELMy H-mode plasmas for the same collisionality. The hybrid plasmas mostly have no or very low gas fuelling. However, the ELM size in these plasmas is strongly reduced when

a small amount of gas fuelling is applied. Figure 6 illustrates how the ELM size of hybrid discharges may be significantly reduced with gas-fuelling for six selected gas-scan session discharges.

For the development of the hybrid plasmas for JET with the ITER-like wall (ILW) the absolute ELM energies and the ELM energy load to the divertor are important. Figure 7 shows the absolute ELM energy losses versus the pedestal stored energy for both the hybrid and baseline ELMy H-mode plasmas.

For hybrid plasmas, the ELM losses scale linearly with the pedestal stored energy and an offset at vanishing ELM energy is observed. The figure illustrates that, in terms of absolute energy losses, the hybrid plasmas feature slightly larger ELMs than the baseline plasmas. This indicates that the ELMs in the thus-far developed hybrid plasmas in JET might not be compatible with the ILW. However, to ascertain this, local measurements of the peak energy loads on the divertor target are needed. Unfortunately these are not available for the hybrid plasmas in this study. The outer divertor strike point in both the low and high triangularity plasmas is situated close to the divertor pump throat to optimise pumping capacity. This location is not suitable for the infrared thermography diagnostics and therefore local energy load measurements could not be performed.

CONCLUSIONS

Systematic analysis of the ELM losses as a function of the pedestal neoclassical collisionality has been carried out in this paper for steady-state standard ELMy H-mode baseline plasmas and hybrid scenarios. The calculation of pedestal parameters and ELM energy drop have been explained in detail. The negative correlation between the ELM losses with the collisionality as found in [1] for baseline ELMy H-mode plasmas has been reproduced here. However, a similar correlation for the hybrid plasmas is absent; The high triangularity hybrid plasmas show a large variation of normalized ELM size for a given value of collisionality. This can be partly explained by the fact that these plasmas show a strong sensitivity to fuelling and recycling. It has been shown that a relatively small amount of fuelling ($25 \cdot 10^{21}$ e/s) reduced the averaged ELM size by a factor of 5, whereas the pedestal collisionality is not changed much in doing so. This effectively causes a large vertical spread in the normalised ELM size versus ν^*. For the plasma presented here the absolute ELM size is of the same order or above that observed in baseline ELMy H-mode plasma. Nevertheless, an outstanding issues remains that the actual ELM energy loads in the divertor could not be measured, and caution therefore needs to be taken in the development of the hybrid scenario with the ILW. In addition, other issues play a role that may have adverse effects on the ILW compatibility of this scenario.

ACKNOWLEDGMENTS

This work was supported by EURATOM and carried out within the framework of the European Fusion Development Agreement. The views and opinions expressed herein do not necessarily reflect those of the European Commission. The authors kindly acknowledge X. Litaudon, Y. Sarazin, M. Becoulet and G. Huysmans for useful discussions.

REFERENCES

[1]. Loarte A., et al 2003 Plasma Physics and Controlled Fusion **45**

[2]. Green B.J., 2003 Plasma Physics and Controlled Fusion **45**

[3]. Frederici G., et al 2003 Plasma Physics and Controlled Fusion **45** 1523

[4]. Shimida M., et al 2004 Nuclear Fusion **44** 350

[5]. Loarte A., et al Proc. 18th IAEA Fusion Energy Conf. (Sorrento, Italy, 2000)

[6]. Osborne T.H., et al 2000 Plasma Physics and Controlled Fusion **42** A175

[7]. Snyder P.B., et al 2002 Physics Plasmas **9** 2037

[8]. Oyama N., et al 2005 Nuclear Fusion **45** 871

[9]. Hudson B., et al 2010 52nd Annual Meeting of the APS Division of Plasma Physics, November 8-12

[10]. Becoulet M., et al 2003 Plasma Physics and Controlled Fusion **45** A93 - A113

[11]. Zhitlukhin A., et al 2007 Journal of Nuclear Materials **363365** 301307

[12]. Riccardo V., et al 2009 Physica Scripta **T138** 014033

[13]. Sips A.C.C., et al 2002 Plasma Physics and Controlled Fusion **44** B69-83

[14]. Luce T.C., et al 2003 Nuclear Fusion **43** 321-9

[15]. Pasqualotto R., et al 2004 Review of Scientific Instruments **75**

[16]. Beurskens M.N.A., et al 2008 Nuclear Fusion **48**

[17]. Pamela S.J.P., et al 2011 Plasma Physics and Controlled Fusion **53** 054014

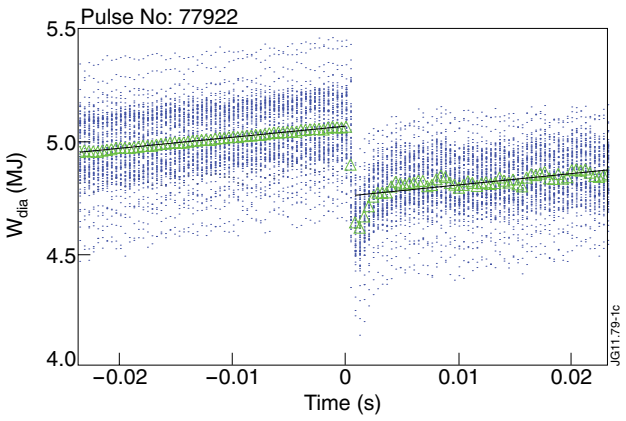

Figure 1: Plasma energy evolution around and ELM for a JET hybrid discharge. Blue points represent the values of W_{dia} synchronised to the ELM crash. For each instant, these values have been averaged over all the ELMs, represented by the green points. A linear regression before and after the ELM crash has been performed. The ELM energy yields from the dierence between the values of the regression line before and after the crash.

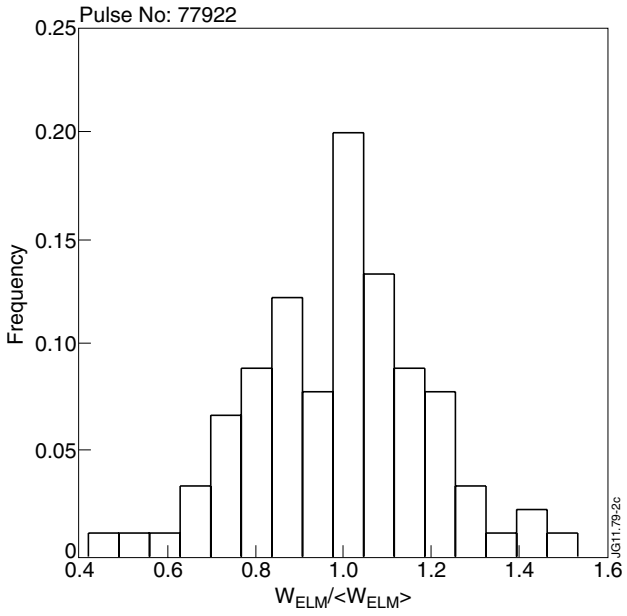

Figure 2: Histogram of the frequency of the ELM energy loss for a single JET hybrid discharge. A sample of 100 ELMs has been used with a standard deviation of 20%.

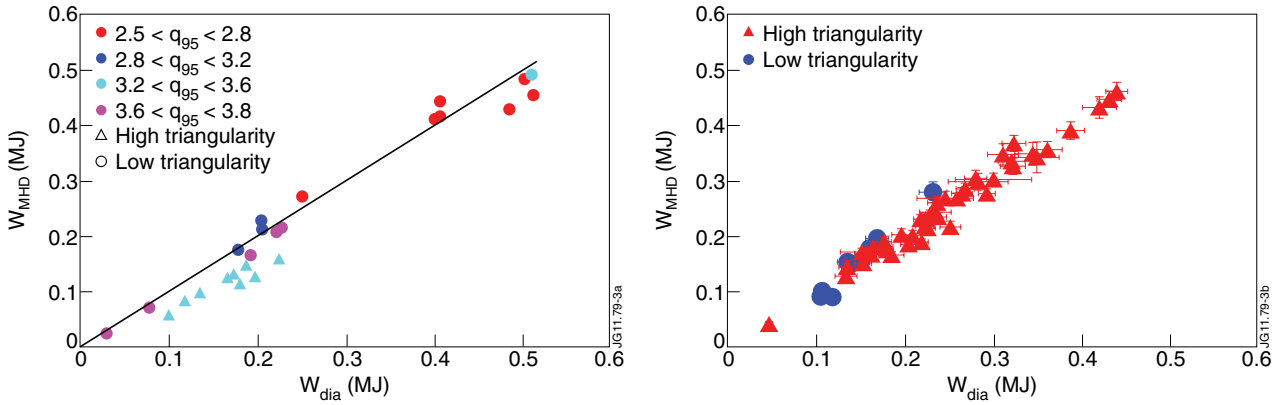

Figure 3: ELM losses from W_{dia} and W_{MHD} for the scenarios analysed in this paper. Triangles represent high triangularity discharges and circles low triangularity discharges.

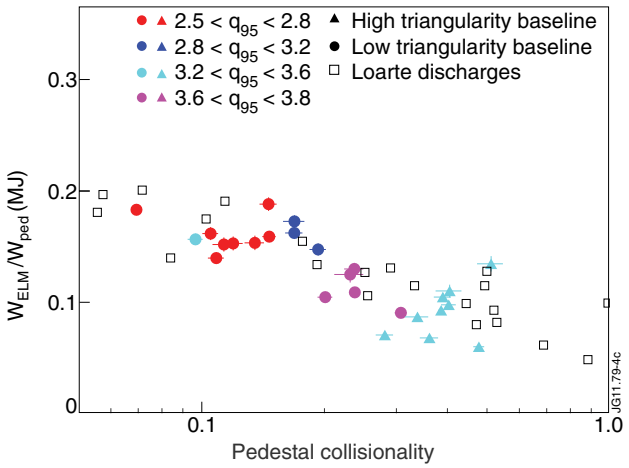

Figure 4: Normalized ELM energy losses versus pedestal plasma collisionality for new JET baseline discharges (closed symbols). Comparison is made with the discharges analysed in [1] (open symbols).

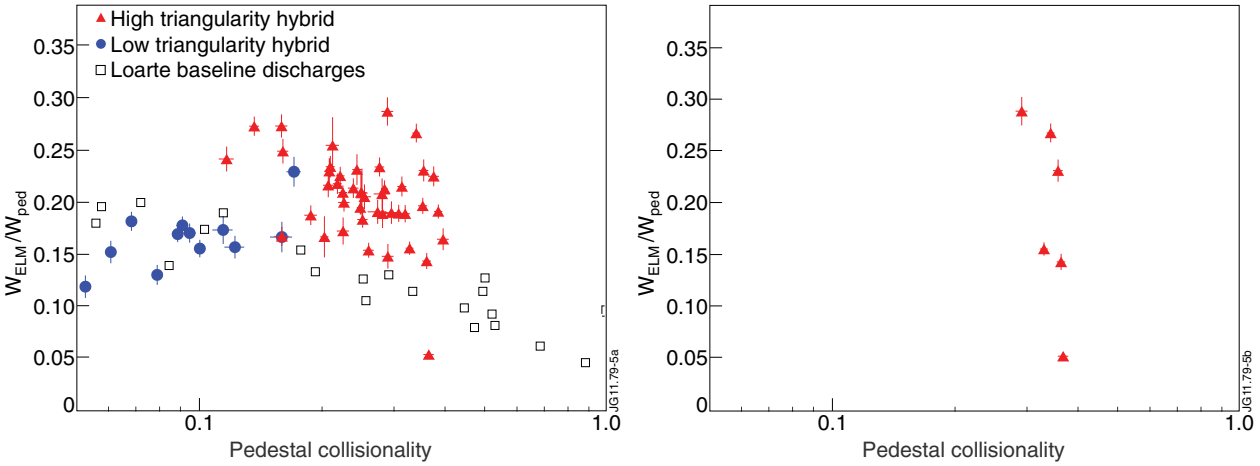

Figure 5: Left: ELM losses versus collisionality for JET hybrid discharges (closed symbols). Comparison is made with baseline plasmas (open symbols). Right: selected gas-scan discharges.

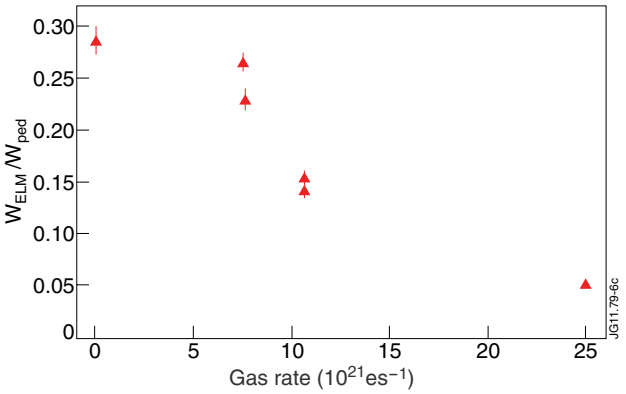

Figure 6: ELM losses versus gas-rate for six JET hybrid discharges atSection 1 0:35: 75954, 75964, 75963, 75962, 74746 and 76748

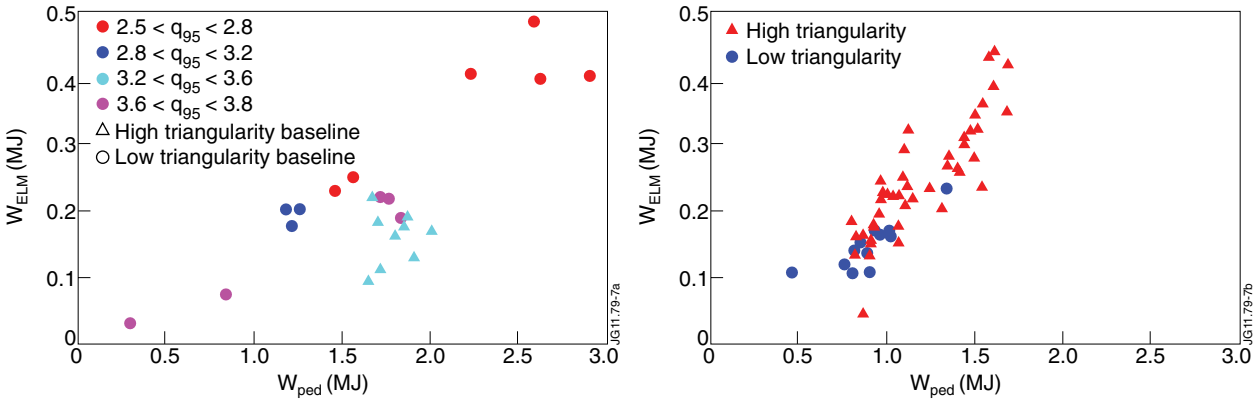

Figure 7: Absolute ELM losses versus pedestal stored energy for baseline (left) and hybrid (right) discharges.